Fermilab FERMILAB-Conf-01/052-E CDF May 2001

SEARCHES FOR SUPERSYMMETRY AT THE TEVATRON

MARY R.M. BISHAI
Fermi National Accelerator Laboratory, Batavia, IL 60510-0500, USA
E-mail: bishai@fnal.gov

We review current experimental results of searches for Supersymmetry (SUSY) at the Fermilab Tevatron Collider using the Run I data collected during 1992-1996. New results from the CDF detector in the jets + missing E_t and lepton-photon channels are presented. Recent results from model independant searches at D0 using the SLEUTH algorithim are reviewed. We discuss the prospects for supersymmetry searches at Run II of the Tevatron, scheduled to start in March, 2001.

1 Introduction

The electrically neutral part of the scalar Higgs field potential within the standard model (SM) can be written as: [1]

$$V = m_H^2|H|^2 + \Lambda|H|^4 \quad (1)$$

There are large radiative corrections, $\delta(m_H^2)$, to m_H^2 from all particles that couple to the Higgs field. These corrections are quadratically divergent in the standard model.

In the Minimal SuperSymmetric extension to the standard model (MSSM), for each fermion there exists a supersymmetric boson partner and vice versa. In addition, there are 2 Higgs doublets corresponding to 5 Higgs particles. The mass of the lightest Higgs is < 130 GeV. The resulting spectrum of particles is given in Table 1.

The addition of supersymmetric partners to the standard model cancels the quadratic divergences in $\delta(m_H^2)$, and leads more naturally to a low-mass Higgs, especially when the masses of the supersymmetric partners are < 1 TeV. Experimentally, this implies that direct observations of such particles could be possible at the FermiLab Tevatron, which operates at a center-of-mass energy of $\sqrt{s} = 1.8$ TeV.

1.1 MSSM phenomenology and implications for experimental signatures

Constructing the MSSM using renormalizable interactions, gauge invariance and Baryon-Lepton (B-L) number conservation, suggests a new symmetry, $R-parity$ with a quantum number, R_p: [2]

$$R_p = (-1)^{3(B-L)+2S} = 1(-1) \text{ for SM particles (SUSY partners)} \quad (2)$$

If $R-parity$ is conserved then SUSY particles can be produced in pairs in collider experiments and decay to stable final state particles, the Lightest SUSY Particle (LSP). If the stable LSP is neutral and colorless, it also becomes

Table 1. Spectrum of particles in the MSSM extension to the Standard Model

Standard Model particle	**SUSY partner**
quarks, q	squarks, $\tilde{q}_{L,R}$
leptons l, ν	sleptons $\tilde{l}_{L,R}$, $\tilde{\nu}_L$
gluons, g	gluinos, $\tilde{g}$
neutral gauge bosons, γ, Z and scaler fields h, H, A	Neutralinos, $\tilde{\chi}^0_{1,2,3,4}$
Charged $W^{\pm}$ bosons and charged Higgs $H^{\pm}$	Charginos, $\tilde{\chi}^{\pm}_{1,2}$

a candidate for dark matter. Since the neutral LSP interacts weakly, it's experimental signature is missing energy in the detectors.

The LSP can be unstable if $R-parity$ is not conserved. In B-violating decays the experimental signature involves multiple jets with little or no missing energy, while L-violating signatures involve multilepton events.

Supersymmetry is a broken symmetry at the electroweak scale. There are several MSSM models that are based on different mechanisms of symmetry breaking and each predicts different experimental signatures. If the symmetry breaking is global, the LSP is then a massless goldstone fermion, the goldstino. In models where the symmetry is broken locally, and gravity is the symmetry-breaking mechanism, the goldstino becomes the longitudinal component of the massive *gravitino* with spin 3/2. The two models most often used to interpret experimental data are:

Minimal Super Gravity (mSUGRA). Supersymmetry breaking occurs at the GUT scale $\sim 10^{16}$ GeV. The gravitino is massive, but its couplings are gravitational in strength, and it therefore plays no role at colliders. The LSP is the lightest SM superpartner and experimental signatures depend on next lightest superpartner (NLSP) masses, and whether $R-parity$ is conserved.

Gauge Mediated Supersymmetry Breaking (GMSB). The SUSY breaking scale is low $\sim$ 100 TeV, the gravitino is therefore light and becomes the LSP. Experimental signatures are γ/τ enriched final states with missing E_t

$$\tilde{\chi}^0_1 \to \gamma\tilde{G},\ \tilde{\tau} \to \tau\tilde{G} \tag{3}$$

1.2 SUSY searches at the Fermilab Tevatron

The Tevatron is a $p\bar{p}$ collider located at the Fermi National Accelerator Laboratory in Batavia, IL, U.S.A. Protons and antiprotons are accelerated to a final energy of $0.9-1.0$ TeV in several stages. The final stage of acceleration happens in the Tevatron ring, a circular superconducting accelerator 4 miles in circumferance. Proton-antiproton collisions take place in 2 areas of the Tevatron ring, where the CDF [3] and D0 [4] detectors are located.

The kinematics of hadronic collisions are those of a hard scattering of constituent quarks, antiquarks and gluons, and therefore $\sum E$, $\sum \vec{\mathbf{P}}$ are unknown. However, ignoring incident gluon radiation, the total energy *transverse* to the beam direction is $\sum \mathbf{E_t} = 0$. As a consequence, experimental searches for SUSY signatures at the Tevatron use selection criteria based on the transverse energy and momentum.

The predicted cross-sections for the production of SUSY particles at the Tevatron depend on the model, and fall in the range $10 - 10^5$ fb. Despite the large range of predictions, the cross-sections for most SM processes at the Tevatron are orders of magnitude larger. Multijet, bottom and W/Z production cross-sections are in the range $10^7 - 10^{12}$ fb, and are the major underlying backgrounds to SUSY signatures. The total integrated Run I luminosity for the D0 and CDF detectors is approximately 120 pb^{-1}.

1.3 The CDF and D0 detectors

The innermost component of the CDF detector for RUN I is a 4-layer Si microstrip detector, 51cm long with 60 % acceptance and an impact parameter resolution of $\sigma_d = 17\mu$m. This is followed by a series of drift chambers in a 1.4T solenoid field. The combined momentum resolution of the tracking chambers is $\sigma_P/P < 0.001P$. Hadronic and electromagnetic (EM) sampling calorimeters are located outside the magnet, arranged in a projective tower geometry with $\Delta\eta \times \Delta\phi = 0.1 \times 0.3$ *or* 0.1 [a]. The inner electromagnetic sectors of the calorimeter towers have lead absorbers with interspersed scintillator/proportional wire chambers (PWC) followed by steel-scintillator/PWC modules for the hadronic calorimeter. A shower-max detector is used to measure the spatial position of the EM shower maximum. The energy resolutions of the EM and hadronic calorimeters are $\Delta E/E \sim 14\%/\sqrt{E}$ and $50\%/\sqrt{E}$, respectively. A system of muon detectors, composed of proportional chambers and steel absorber, is installed outside the calorimeter.

The Run I D0 detector tracking volume consists of a series of drift chambers and a transition radiation detector (for electron identification). The tracking volume has no magnetic field. D0 Run I tracking resolutions are $\delta\phi = 2.5$ mrad and $\delta\theta = 28$ mrad. A liquid-Argon sampling calorimeter with excellent coverage encloses the tracking volume. The calorimeter is arranged in pseudoprojective towers with $\Delta\eta \times \Delta\phi = 0.1 \times 0.1 (0.5 \times 0.5$near showermax). The absorbers are depleted Uranium for the electromagnetic and fine-hadronic sections, and Cu/Steel in the coarse-hadronic section. The energy resolution

[a] Production angles are often described using the *pseudorapidity*, η, where

$$\eta = -1/2 \ln \tan \theta/2 \approx 1/2 \ln(E + P_z)/E - P_z) \text{ (for } m << P_t) \quad (4)$$

m is the mass of the particle, $P_{z,t}$ are the components of the particle's momentum parallel and transverse to the beam direction, and θ and ϕ are the polar and azimuthal production angles.

of the D0 calorimeter is $\Delta E/E \sim 15\%/\sqrt{E}$ (EM) and $50\%/\sqrt{E}$ (hadronic). The muon system consists of planes of proportional drift tubes in front of and behind magnetized iron toroids. The μ momentum resolution is $\sigma(1/p) = 0.2(p-2)/p^2$.

2 SUSY searches in Run I

The interpretation of the experimental results of a search for a particular SUSY signature is model dependent and is often given as a limit on some parameters for a given set of assumptions. The MSSM has 124 independent parameters; 18 SM + 105 new + 1 Higgs. These SUSY parameters are

1. μ the higgsino mixing paramter
2. $v_{u,d}$ the vacuum expectation values of the Higgs doublets coupling to the u and d quarks, respectively, parameterized by the ratio $\tan\beta = v_u/v_d$ with $v_u^2 + v_d^2 = 4M_W^2/g^2 = 246$ GeV^2.
3. Mass of the pseudoscalar Higgs, M_A, and masses of the sparticles, $M_{\tilde{q}}$, $M_{\tilde{l}}$ and gauginos, $M_{\tilde{\chi}}$.
4. λ_f, where $f = u, d, e$ are the Higgs-fermion Yukawa couplings.

mSUGRA unifies the particle masses and couplings at the GUT scale thereby reducing the mass and coupling parameters to only 3. The mSUGRA parameters are M_0 and $M_{1/2}$, the common scaler and gaugino masses, and A_0, the common trilinear coupling. Some of the CDF and D0 searches are interpreted in the framework of SUGRA-inspired models [2], and use 5 main input parameters; $M_{\tilde{q}}$,$M_{\tilde{g}}$,M_{A_0}, $\tan\beta$, $|\mu|$ and sign(μ), where $M_{\tilde{q}}$ is the mass of the first 5 degenerate squarks. In SUGRA, the masses of the sleptons can be derived from $M_{\tilde{q}}, M_{\tilde{g}}, M_Z$ and β. The properties of $\tilde{\chi}_i^{\pm}$ and $\tilde{\chi}_i^0$ are determined from the $M_0, M_{1/2}, \tan\beta$ and μ values.

2.1 Trilepton and Tetralepton signatures

In mSUGRA the gauginos ($\tilde{\chi}$s) are usually lighter than the gluinos or squarks, and therefore may be the only particles accessible at the Tevatron. Multilepton signatures from the direct production and decay of gauginos arise from the following decay steps:

$$p\bar{p} \to \tilde{\chi}_1^{\pm}\tilde{\chi}_2^0,\ \tilde{\chi}_1^{\pm} \to \tilde{\chi}_1^0 l^{\pm}\nu,\ \tilde{\chi}_2^0 \to l^+l^-\tilde{\chi}_1^0 \tag{5}$$

The branching ratios depend on mass splittings and are highly model dependent. When $\tilde{\chi}_2^0 \to \tilde{l}l$, $\tilde{l} \to l\tilde{\chi}_1^0$, and either $\Delta M(\tilde{\chi}_2^0, \tilde{l})$ or $\Delta M(\tilde{\chi}_1^0, \tilde{l})$ is small, then the lepton is too soft to be detected. For the case where $\Delta M(\tilde{\chi}_2^0, \tilde{\chi}_1^0) > m_{Z,h}$, real Zs are produced, and the events are indistinguishable from SM $Z \to ee$ background. Any decays of $h \to b\bar{b}$ reduce the leptonic branching fractions.

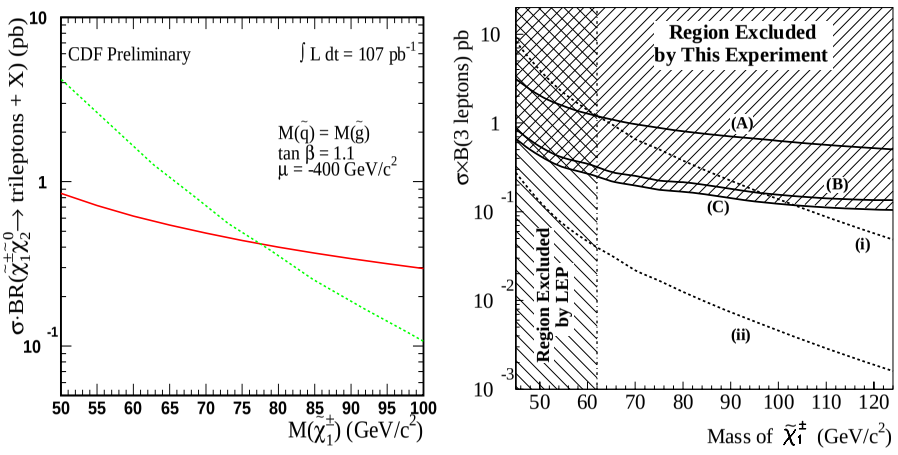

Figure 1. Production cross section times branching ratio to leptons for chargino-neutralino production as a function of chargino mass within the SUGRA framework from CDF (left) and D0 (right). The dashed lines are the theoretical limits for M_0 and $M_{1/2}$. The solid lines are the 95% C.L. limits of exclusion (space above). The results from D0 are for (A) the 1992-1993 data, (B) the limit from 1994-1995 data,and (C) the combined limit.

The trilepton signatures are considered the golden mode for SUSY since SM backgrounds are small. Possible sources of SM backgrounds are $\gamma^*, Z, \Upsilon, J/\psi$ production, and decay to ll and an extra fake lepton + $\not\!\!E_t$, diboson production with decays to leptons and, semileptonic decays of b/c pairs and a false extra lepton.

Both CDF and D0 conducted a search for events containing eee, $ee\mu$, $e\mu\mu$, $\mu\mu\mu$ [5] [6]. The selection criteria involved transverse momentum requirements on the leptons of $P_t > 5 - 11$ GeV, $\not\!\!E_t > 10 - 15$ GeV, topological criteria on the opening angles between the leptons and the $\not\!\!E_t$, and restriction on ll invariant mass. CDF also applied an opposite charge requirement on two of the leptons. Both experiments find no candidates. Expected backgrounds are 1.2 ± 0.2 and 1.3 ± 0.4 for CDF and D0, respectively. The limits on $\sigma.\mathrm{Br}(\tilde{\chi}_1^{\pm}\tilde{\chi}_2^0 \rightarrow trileptons + X)$ as a function of chargino mass are shown in Figure 1.

mSUGRA models with $R - parity$ violation also give rise to trilepton signatures from the leptonic decay of the LSP, which in this case is the lightest neutralino

$$p\bar{p} \rightarrow sparticles \rightarrow \tilde{\chi}_1^0\tilde{\chi}_1^0 + X, \quad \tilde{\chi}_1^0 \rightarrow \nu l^+ l^- \tag{6}$$

The $\tilde{\chi}_1^0 \rightarrow \nu l^+ l^-$ branching fraction depends on the strength of the $\not\!\!R_p$ couplings, λ_{ijk}, $i,j,k = 1,2,3$ for the 3 lepton families. Since experimental searches are more sensitive to decays with the highest e and μ multiplicities, the results are most sensitive to λ_{121} and least sensitive to λ_{233} (τs). Figure

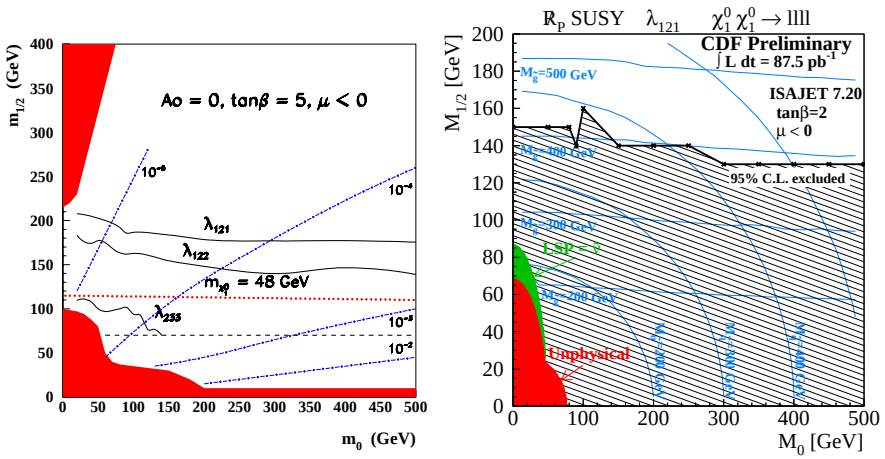

Figure 2. Results from CDF(left) and D0(right) on searches for $R-parity$ violation in multilepton final states. The D0 result shows exclusion contours at the 95% C.L. limits for $A_0 = 0, \mu < 0$, $\tan\beta = 5$ for the case of finite $\lambda_{121}, \lambda_{122}$ and λ_{233} couplings. The CDF exclusion contours are shown for different values of gluino and squarks masses and $A_0 = 0, \mu < 0$, and $\tan\beta = 2$. In both plots the solid regions are excluded because of unphysical behavior such as no EW symmetry breaking.

2 shows the experimental limits in the M_0, $M_{1/2}$ plane from D0's reinterpretation of their trilepton results where the fourth lepton was undetected for a given value of $A_0, \tan\beta$ and μ [7]. A CDF search for all 4 leptons [8] by loosening the selection criteria on the trilepton search, and requiring all 4 leptons to be detected, yields 1 $ee\mu\mu$ event, with an expected background of 1.3 ± 0.4. The CDF exclusion contours in M_0, $M_{1/2}$ plane are also shown in Figure 2.

2.2 Searches in modes containing jets, leptons and $\not\!\!E_t$.

Squarks and gluinos couple strongly $(SU(3)_c)$ to quarks and gluons, and could therefore have large production cross-sections at Tevatron, depending only on their masses. They could also be produced in association with $\tilde{\chi}$ which can be kinematically favorable:

$$p\bar{p} \to \tilde{g}\tilde{g} \quad p\bar{p} \to \tilde{q}\bar{\tilde{q}} \quad p\bar{p} \to \tilde{q}\tilde{\chi}_1^{\pm} \quad p\bar{p} \to \tilde{g}\tilde{\chi}_2^0 \tag{7}$$

Decays of squarks/gluinos depend on their electroweak couplings to charginos/neutralinos and their mixing, which also determines their masses. Several decay scenarios are possible depending on the mass hierarchy. If $M_{\tilde{q}} > M_{\tilde{g}}$, then

$$\tilde{q} \to \tilde{g}q, \ \tilde{g} \to q\bar{q}\tilde{\chi}_2^0 \text{ or } q\bar{q}'\tilde{\chi}_1^{\pm} \text{ or } t\tilde{t}^* \text{ or } t\bar{t} \text{ or } g\tilde{\chi}_1^0 \tag{8}$$

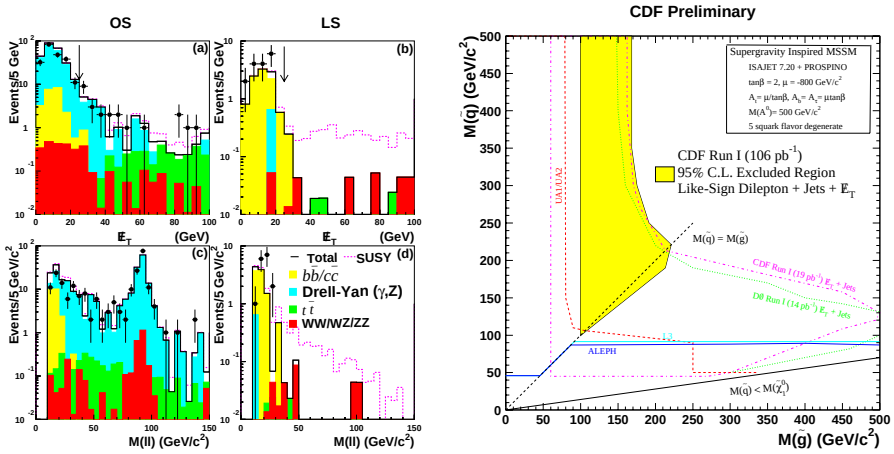

Figure 3. CDF results on squark gluino searches in $l^{\pm}l^{\pm}\ jj$. On the left are the distributions for RUN I data (points with error bars), and backgrounds (solid histograms), and the expected signal (dashed line). On the right are the corresponding exclusion contours in the squark-gluino mass plane.

If $M_{\tilde{q}} < M_{\tilde{g}}$, then

$$\tilde{g} \to \tilde{q}q,\ \tilde{q}_{L,R} \to q\chi_i^0,\ \tilde{u}_L \to d\chi_i^+,\ \tilde{d}_L \to u\chi_i^-, \tag{9}$$

The experimental signatures for squark/gluino production and decay are therefore similar to $\tilde{\chi}\tilde{\chi}$ production, with the addition of jets from quark decays.

CDF searches for squark/gluinos in the signature mode $l^{\pm}l^{\pm}\ jj\ \not\!\!E_t$: [9]

$$p\bar{p} \to \tilde{g}\tilde{g} \to (q\bar{q}'\tilde{\chi}_1^{\pm})(q\bar{q}'\tilde{\chi}_1^{\pm}) \to q\bar{q}(l^{\pm}\nu\tilde{\chi}_1^0)q\bar{q}'(l^{\pm}\nu\tilde{\chi}_1^0) \tag{10}$$

In certain regions of the MSSM parameter space, up to 30% of dilepton events from squark/gluino production can be like-sign (LS). Experimentally, the LS signature has smaller SM backgrounds, as shown in Figure 3. CDF requires 2 isolated leptons (e or μ) with transverse energy, $E_t >$ 5,11 GeV. The dileptons must be separated from each other, and from the two jets, to reject b backgrounds. The selection on the 2 jets are $E_t > 15$ GeV and $|\eta| < 2.4$. In addition, the event is required to have $\not\!\!E_t > 25$ GeV. The distribution of CDF RUN I data, background and expected signal for opposite sign (OS) and LS events, and the exclusion contours as a function of squark and gluino masses are shown in Figure 3. The data match SM expectations.

D0 has searched for squarks and gluinos in the dilepton + $jets$ + $\not\!\!E_t$ [10] signature mode. No events were found beyond background expectations.

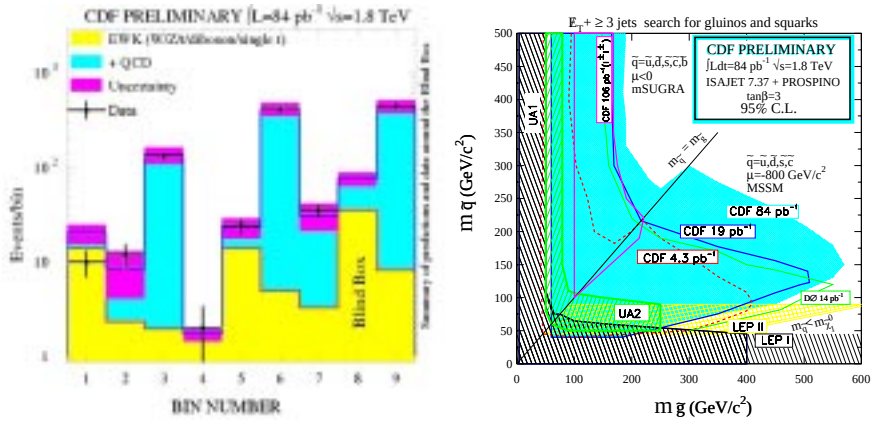

Figure 4. CDF results on squark gluino blind searches in $jets + \not\!\!E_t$. On the left is the comparison of SM prediction and data in bins around the blind box. On the right is the 95% C.L. contour in the squark-gluino mass plane. Results from previous searches are also shown.

2.3 CDF "blind" search for squarks/gluinos in $\geq 3jets + \not\!\!E_t$.

Searches for signatures with $jets + \not\!\!E_t$ have large SM backgrounds such as diboson production and decay, $WZ + jets$, $W \rightarrow l\nu + jets$, multijets where $\not\!\!E_t$ comes from mismeasurement of jet energy, $t\bar{t}$ production and hadronic decay. A new search from CDF compares a normalized background and any SUSY signature in the mode $\geq 3jets + \not\!\!E_t$. Several kinematic variables are used to select the region in phase space where the SUSY signature is most likely to be: $\not\!\!E_t$, the sum of the transverse energies of 2 jets and of $\not\!\!E_t$ ($H_t = E_t^{2^{\rm nd}{\rm jet}} + E_t^{3^{\rm rd}{\rm jet}} + \not\!\!E_t$), and the number of isolated tracks in the event (N_{trk}^{iso}).

Outside of the signal region, backgrounds are studied and normalized to MC. MC predictions for $Z/W + \geq N_{jets}$ backgrounds are normalized using CDF data on $Z \rightarrow ee + 2jets$. The multijet background predictions are generated using enhanced leading order HERWIG calculations [11], with the measured trigger efficiencies folded in. The multijet distributions are then compared to data and rescaled. The resummed theoretical $\sigma_{t\bar{t}} = 5.06^{+0.13}_{-0.36} pb$ for $m_{top} = 175$ GeV is used to normalize the MC $t\bar{t}$ background predictions to the data luminosity.

The selections are then optimized to increase sensitivity to the SUSY signatures. The final step of the analysis is to compare the SM predictions and observed data in the interesting region. The SM predictions in the "blind" box are 76 ± 13 events, and 74 events are observed. Figure 4 shows the CDF SM signal and background in the 9 kinematic regions selected, and the exclusion contours in the squark-gluino mass plane.

2.4 Light Stop search

The $\tilde{t}$ mass degeneracy is strongly broken since the splitting is proportional to the top mass:

$$\tilde{t}_1 = \cos\theta_{\tilde{t}}\tilde{t}_L + \sin\theta_{\tilde{t}}\tilde{t}_R, \quad \tilde{t}_2 = -\sin\theta_{\tilde{t}}\tilde{t}_L + \cos\theta_{\tilde{t}}\tilde{t}_R \tag{11}$$

If there is sufficiently large mixing the lightest stop, $\tilde{t}_1$, could even be lighter than the charginos, and decay as follows:

$$p\bar{p} \to \tilde{t}_1\bar{\tilde{t}_1} \to (\tilde{\chi}_1^0 c)(\tilde{\chi}_1^0 \bar{c}) \tag{12}$$

On the other hand, if $\tilde{t}_1 \to \tilde{\chi}_1^{\pm} b$ is kinematically allowed, then

$$p\bar{p} \to \tilde{t}_1\bar{\tilde{t}_1} \to (\tilde{\chi}_1^+ b)(\tilde{\chi}_1^- \bar{b}) \to ee\ jets\ \not\!\!E_t \tag{13}$$

If the $\tilde{t}_1$ mass is in the range 100 - 150 GeV, the direct production cross-section may be too small, but one could look for stop in top decays, where

$$p\bar{p} \to t\bar{t} \to (\tilde{t}_1\tilde{\chi}_1^0)(\bar{\tilde{t}}_1\tilde{\chi}_1^0) \quad \tilde{t}_1 \to b\tilde{\chi}_1^{\pm},\ \tilde{\chi}_1^{\pm} \to l\nu\tilde{\chi}_1^0 \text{ or } q\bar{q}'\tilde{\chi}_1^0 \tag{14}$$

D0 has searched for light stop [12] in the scenario outlined in Equation 12 by looking for 2 jets with $E_t > 30GeV$, and $\not\!\!E_t > 40GeV$. The jets are required to be acollinear, $90^o < \Delta\phi_{jj} < 165^o$; $10^o < \Delta\phi_{\not\!\!E_t,j_i}$, $\Delta\phi_{\not\!\!E_t,j_1} < 125^o$, $10^o < \Delta\phi_{\not\!\!E_t,j_i}$. The number of observed events is 3 with an expected background of 3.5 ± 1.2.

Using the random grid search program, D0 [13] has also looked for light stop production in the mode of Equation 13. SM backgrounds are $t\bar{t}$ and $W/Z \to llX$. Only 2 events were observed events, where 4.4 ± 0.8 events expected.

CDF searches for the stop signature [14] from Equation 14 using jet flavor tagging and the standard isolated $l + \geq 2\ jets + \not\!\!E_t$ events in the $t\bar{t}$ search analysis. The analysis selections are revised to improve sensitivity to kinematics of the smaller mass $\tilde{t}_1$: lower P_t, E_t^{jets}, multiplicity, and no peak in $M_t(l + \not\!\!E_t)$. The number of observed events in CDF data is 9 with an expected background of 9.5.

Thus, there is no evidence for the existence of a light $\tilde{t}$ in Run I data.

2.5 Search for Non Standard Higgs

In 2 Higgs doublet models, where one couples to u and the other to d, there are 5 physical Higgs bosons: 2 neutral scalers h^0, H^0, a neutral pseudoscalar, A^0 and 2 charged scalers $H^{\pm}$. CDF searches for neutral Higgs [15] within MSSM in

$$p\bar{p} \to b\bar{b}\varphi \to b\bar{b}(b\bar{b}) \quad (\varphi = h, H, A) \tag{15}$$

The signature is $\geq 4jets$, where 3 of the jets are b-tagged using the CDF jet-tagging algorithm. The distributions in data distributions agree with SM expectations. The results are shown in Figure 5.

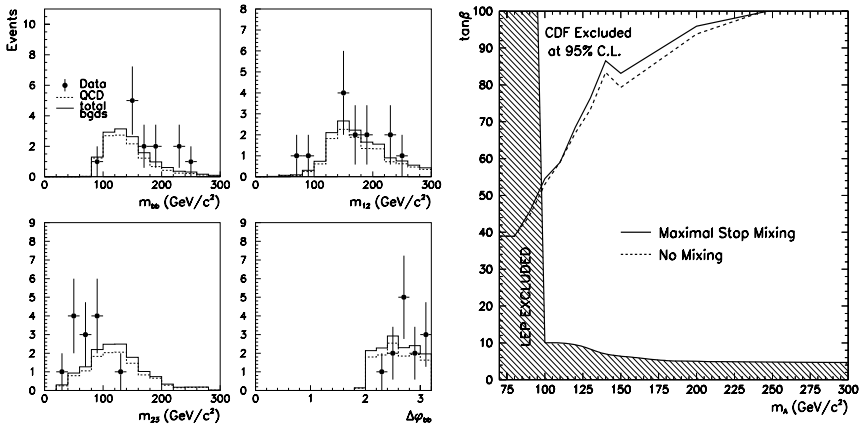

Figure 5. CDF results on neutral MSSM Higgs boson search. Data (points with error bars) and background distributions (dashed and solid histograms) are shown on the left for various kinematic distributions: M_{bb} the invariant mass of the tagged b jets, M_{12} and M_{23} the invariant masses of the 3 highest-E_t jets, and $\Delta\phi$ the angle between the two b-jets. The 95% C.L. excluded region in the m_A, $\tan\beta$ plane is shown on the right.

$H^{\pm}$ coupling to $d(u)$ or $\nu(l)$ is proportional to $m_{fermion} \times \tan\beta(\cot\beta)$. If $\tan\beta$ is very large or very small, and the decay is kinematically allowed, then $B(t \to Hb)$ could be significant compared to $B(t \to Wb)$, and the $H^{\pm}$ would decay:

$$(1)\ H \to c\bar{s}, \quad (2)\ H \to Wb\bar{b}, \quad (3)\ H \to \tau\nu_{\tau} \tag{16}$$

The signature dependens on specific model parameters. D0 has searched for the disappearance of SM $WWbb$ signature [16] in top $l+jets$ events. This search is particularly sensitive to decays (1) and (3). The number of observed events is $N_{obs} = 30$. Given $\sigma(t\bar{t}) = 5.5$pb, $m_t = 175$ GeV, and $B(t \to Wb) = 1$, the expected signature without any contribution from $H^{\pm}$ is 30.9 ± 4.0.

2.6 Signatures with $\gamma\gamma$

Photon enriched signatures arise in GMSB models. For example, slepton production with a light gravitino:

$$p\bar{p} \to \tilde{e}\tilde{e}X \to (e\tilde{\chi}_1^0)(e\tilde{\chi}_1^0) \to e(\gamma\tilde{G})e(\gamma\tilde{G}) \tag{17}$$

A similar signature arises in models where $\tilde{\chi}_2^0$ has a large photino component, and decays into $\gamma\tilde{\chi}_1^0$:

$$p\bar{p} \to \tilde{e}\tilde{e}X \to (e\tilde{\chi}_2^0)(e\tilde{\chi}_2^0) \to e(\gamma\tilde{\chi}_1^0)e(\gamma\tilde{\chi}_1^0) \tag{18}$$

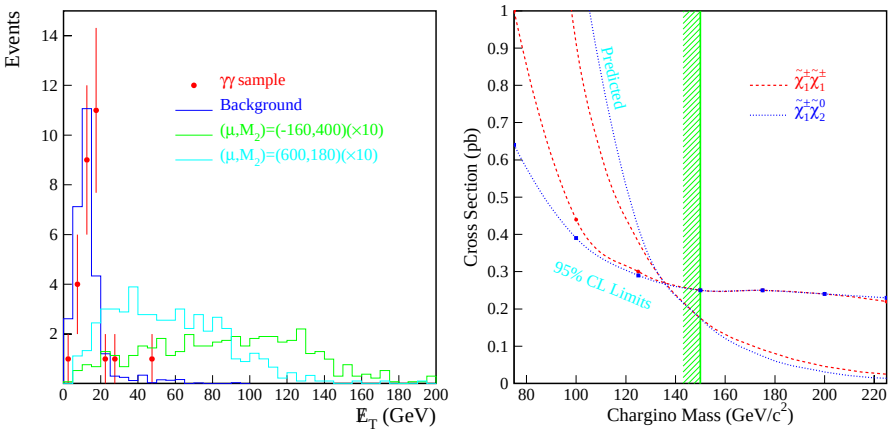

Figure 6. Diphoton search results from D0. On the left is $\not\!\!E_t$ distributions of $\gamma\gamma$ data (points with error bars) and SM background expectations (solid histogram). The dashed histograms are the expected distributions from two representative points in the supersymmetry parameter space. On the right are the measured 95% C.L. upper limits and predicted theoretical crossections for gaugino production as a function chargino mass. The vertical hatched line is the 95% C.L. lower limit on the chargino mass determined using the total crossection for all gaugino pair production and all possible μ values.

D0 has searched for $\tilde{\chi}^0\ \tilde{\chi}^{\pm}$ production [17] where $\tilde{\chi}^0_1 \rightarrow \gamma\tilde{G} \Rightarrow \gamma\gamma\not\!\!E_t X$. The trigger is an EM cluster with $E_t > 15$ GeV, 1 jet with $E_t > 10$ GeV, and $\not\!\!E_t > 14$ GeV. The photon is identified as an isolated EM shower with no matching track or hits in the tracking chambers. The selection criteria on the 2 photons are $E_t^{\gamma_1} > 20GeV$, $E_t^{\gamma_2} > 12GeV$. Events also require $\not\!\!E_t > 25$GeV and one reconstructed vertex. The SM backgrounds for this mode are $W+\gamma$, $W + jets$ and $Z \rightarrow ee$ where electrons are misidentified as photons. The results of the D0 diphoton search are shown in Figure 6. The data are in good agreement with SM predictions.

2.7 Search for new physics in Lepton-Photon events

CDF conducted a model independent search for the production of new massive particles that would cascade decay to $\gamma + W/Z$, $W/Z \rightarrow lX$ [18]. These $\gamma - l$ (e or μ) events are categorized by the number of final state particles:

Two body: 1 photon 1 lepton and no additional photons or leptons. The lepton and photon are required to be nearly back to back; $\Delta\phi_{l\gamma} > 150$

Multi body $l\gamma\not\!\!E_t$: Multi-body final states with $\not\!\!E_t > 25$ GeV.

Multi body multi lepton: Multibody final states resulting in multilepton signatures.

Table 2. Preliminary CDF photon-lepton results and probabilities that N_{SM} can fluctuate to $N_{observed}$.

Category	**Predicted** N_{SM}	**Observed** N_o	$P(N_{SM} \geq N_o)$ %
All $l\gamma X$	-	77	-
Two-Body $l\gamma X$	24.9 ± 2.4	33	9.3
Multi-Body $l\gamma X$	20.2 ± 1.7	27	10.0
Multi-Body $ll\gamma X$	5.8 ± 0.6	5	61.0
Multi-Body $l\gamma\gamma X$	0.02 ± 0.02	1	1.5
Multi-Body $l\gamma \not\!\!E_t X$	7.6 ± 0.7	16	0.7

Multi body multi photon: Multibody final states producing several photons.

SM backgrounds for $n(l)+n(\gamma)$ events arise from $W/Z+\gamma$ production, $l+jet$ production where the jet is misidentified as a γ, $Z \to ee$ where e is misidentified as a γ, π/K punchthrough/decay misidentified as prompt μ and b/c semileptonic decays. The inclusive event rates of each category are compared with SM predictions. The results of the searches in different categories are listed in Table 2 and an excess is observed in the $l\gamma \not\!\!E_t X$ sample. Since in the context of this analysis, 5 mostly independent comparisons with the SM were made using the same collection of data, the likelihood is high that one of the outcomes with 1% probability will occur. The observed excess is therefore less significant than the indicated 0.7% probability and does not provide a compelling case for new physics. This analysis sets up an important Run II a priori search.

2.8 SLEUTH: Development of a model independent algorithm for detection of new high-P_t physics

In general, a signature for new physics is a region of variable space in which $P(N_{bkgd} \geq N_{obs})$ is small. New physics is also expected to populate regions of high P_t. SLEUTH [19] is a new quasi-model-independent search algorithm for new physics at high P_t that has been developed at D0. Given a desired final state, a rule is constructed that identifies a set of relevant kinematic variables. The background expected in the phase space defined by these variables is estimated, and the probability that the number of observed events can be interpreted as a background fluctuation is calculated. The sensitivity of the method is determined by applying it to a series of hypothetical similar experiments.

A search for new physics in $e\mu X$ data at D0 was conducted using SLEUTH [19] [20]. SM backgrounds for these signatures include events with a true muon and a jet misidentified as an electron, $Z \to \tau\tau$, $\gamma^* \to \tau\tau$, WW and $t\bar{t}$. The results are listed in Table 3. There is no evidence for new physics.

Table 3. Summary of D0 SLEUTH searches for new physics on all final states within the $e\mu X$ data sample.

Dataset	**Variables**	**Probability**
$e\mu\not{E}_t$	P_T^e, $\not{E}_t$	0.14
$e\mu\not{E}_t$ 1 *jet*	P_T^e, $\not{E}_t$, P_T^J	0.45
$e\mu\not{E}_t$ 2 *jets*	P_T^e, $\not{E}_t$, P_T^{J2}	0.31
$e\mu\not{E}_t$ 3 *jets*	P_T^e, $\not{E}_t$, $P_T^{J2} + P_T^{J3}$	0.71
Combined		0.72

Table 4. Summary of Tevatron upgrade for Run II.

	Run IB	Run II (Main Injector & Recycler)
Energy	900	1000GeV
Typical Luminosity	$1.6X10^{31}$	$2.0X10^{32}$ cm^{-2} s^{-1}
Integrated Luminosity*	3.2	41.0 pb^{-1}/week
Number of Bunches	6	36
Bunch Spacing	3500	396-132 nsec

3 SUSY searches at the Tevatron in Run II

3.1 Tevatron upgrade

The FNAL accelerator facility has undergone a series of major upgrades which will greatly enhance performance in RUN II. The new Main Injector will provide a larger flux of protons for antiproton production, more intense proton bunches and higher efficiency for acceleration of antiprotons. The Recycler Ring is a new post-accumulator and receptacle for recycled antiprotons from previous collider stores. This upgrade provides more antiprotons for the Tevatron, thereby increasing luminosity. The Run II Tevatron performance upgrades are summarized in Table 4.

3.2 CDF and D0 detector upgrades

The CDF and D0 detectors are also undergoing major upgrades in preparation for RUN II so as to improve the physics reach and take advantage of the accelerator upgrade. Both detectors have new inner silicon tracking detectors and new central trackers. D0 has added a 2T superconducting solenoid in the central region for better determination of momenta and particle identification. Both detectors have completely new data acquisition systems and trigger electronics to accommodate the 132ns bunch crossing time and increased accelerator luminosity.

The inner section of the CDF RUN II silicon detector, SVXII, is comprised of 3 cylindrical barrels with 5 layers of double-sided silicon and a total length of 96 cm for full coverage of the $\pm$30 cm interaction region. In addition to

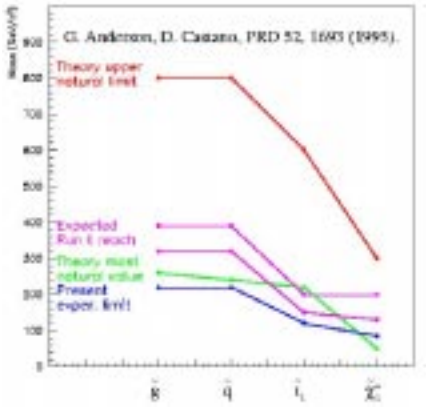

Figure 7. Projections of the Tevatron RUN II reach for several SUSY particles.

SVXII, the Intermediate Silicon Layers (ISL) are an extra layer of Si outside of SVXII at $|\eta| < 1$, and 2 layers at $1.0 < |\eta| < 2$. A single-sided Si layer installed directly on the Be beam pipe (L00) brings the total number of Si layers to 8, and the number of readout channels to over 700,000. A new central outer tracker, the COT is an open-cell drift chamber, with drift times < 100ns, and 30,240 readout channels. New scintillating-tile plug-calorimeters have also been added, and a time-of-flight system between the COT and calorimeter was installed to enhance particle identification.

The new D0 silicon tracker consists of 4 layer barrels of both double and single sided silicon interspersed with double sided disks for better resolution of tracks at high η. The D0 Silicon Tracker has 840,000 readout channels. The central tracking system has 8 layers of 830 μm scintillating-fiber ribbon-doublets, read out with new visible light photon counters (74,000 VLPC channels). There are also new central and forward preshower scintillator strips and with wavelength-shifter fiber readout (6,000 and 16,000 VLPC channels, respectively).

3.3 SUSY reaches in RUN II

There have been many searches in Run I but without evidence for SUSY. In e^+e^- machines, the limits are from kinematics, but the Tevatron reach is currently limited only by luminosity. In Run I, with 0.1 fb^{-1} CDF/D0 results are competitive with LEP for $\tilde{q}$, $\tilde{g}$. In Run II, the factor of 20-200 in luminosity will provide sensitivity to production of Higgs and $\tilde{\chi}$ by about a factor of two beyond the current LEP limits (for combined CDF-D0 results). As shown in Figure 7, the expected reach as a function of sparticle mass is expected to pose a serious challenge to current models.

4 Conclusion

The CDF and D0 collaborations have conducted extensive searches for SUSY in RUN I at the Fermilab Tevatron. Despite the fact that there has been no evidence observed for SUSY, there are still many signatures remaining to be explored in the RUN I data. As shown in Figure 7, the increased luminosity of the Tevatron, and enhanced performance of the upgraded detectors, implies that the new searches will start to probe the theoretically most interesting region. The expected extension of RUN II to an integrated luminosity of 20 fb^{-1} will provide the crucial test of the MSSM Higgs-boson sector. In addition, the emergence of new analysis techniques that are model independent will further facilitate the search for new physics beyond the Standard Model.

Acknowledgments

The author would like to acknowledge the hard work of the CDF and D0 collaborations for their efforts in searching for supersymmetry in RUN I of the Tevatron. The author would particularly like to thank Ray Culbertson for his help, guidance and invaluable instruction.

References

1. S. P. Martin in *Perspectives on Supersymmetry*, ed. G.L. Kane.
2. M. Carena *et al.* in *Perspectives on Supersymmetry*, ed. G.L. Kane.
3. F. Abe *et al.*, *Nucl. Instrum. Methods* A **271**, 387 (1988).
4. S. Abachi *et al.*, *Nucl. Instrum. Methods* A **338**, 185 (1994).
5. F. Abe *et al.*, *Phys. Rev. Lett.* **80**, 5275 (1998).
6. B. Abbott *et al*, *Phys. Rev. Lett.* **80**, 1591 (1998).
7. B. Abbott *et al.*, *Phys. Rev.* D **62**, 071701 (2000).
8. A. Köngeter, Presented at the "Higgs and SuperSymmetry, Search & Discovery" Conference, Gainesville, Florida, March 8-11, 1999.
9. J. P. Done *et al.*, CDF-ANAL-EXOTIC-CDFR-4909 (1999).
10. B. Abbott *et al.*, *Phys. Rev.* D **63**, 091102 (2001).
11. G. Marchesini *et al.*, *HERWIG Version 5.9*, hep-ph/9607393 (1996).
12. S. Abachi *et al.*, *Phys. Rev. Lett.* **76**, 2222 (1996).
13. S. Abachi *et al.*, *Phys. Rev.* D **57**, 589 (1998).
14. T. Affolder *et al.*, *Phys. Rev.* D **63**, 091101 (2001).
15. T. Affolder *et al.*, FERMILAB-PUB-00-258-E, hep-ex/0010052 (2000).
16. B. Abbott *et al.*, *Phys. Rev. Lett.* **82**, 4975 (1999).
17. B. Abbott *et al.*, *Phys. Rev. Lett.* **80**, 442 (1998).
18. T. Affolder *et al.*, CDF-PUB-EXOTIC-CDFR-5569 (2001).
19. B. Abbott *et al.*, *Phys. Rev.* D **62**, 092004 (2000).
20. B. Abbott *et al.*, FERMILAB-PUB-00-304-E, hep-ex/0011071 (2000). Accepted for publication in *Phys. Rev. Lett.*.